

Regular article

The ground state of TiC revisited

Charles W. Bauschlicher Jr.

Mail Stop 230-3, Space Technology Division, NASA Ames Research Center, Moffett Field, CA 94035, USA

Received: 20 March 2002 / Accepted: 27 August 2002 / Published online: 8 October 2003
© Springer-Verlag 2003

Abstract. The ground state of TiC is $^3\Sigma^+$, as predicted by previous configuration interaction calculations. It is shown that there are two low-lying $^1\Sigma^+$ states and that the density functional theory solution corresponds to the higher of the two $^1\Sigma^+$ states.

Keywords: MRCI+Q – Spectroscopic constants – Douglas – Kroll – Hess – Excited states – electron correlation

1 Introduction

We recently computed [1] the spectroscopic constants of the $^3\Sigma^+$ and $^1\Sigma^+$ states of TiC using density functional theory (DFT). With the DFT approaches, the separation between the $^1\Sigma^+$ and $^3\Sigma^+$ states varies with choice of functional, with some functionals yielding a $^1\Sigma^+$ ground state [1, 2]. Configuration interaction (CI) calculations [2, 3] yield a $^3\Sigma^+$ ground state with the $^1\Sigma^+$ state quite low-lying. While it is not too surprising that the DFT and CI approaches might differ on the T_e values, it is surprising that the r_e , ω_e , and dipole moment values for the $^1\Sigma^+$ state are very different at the DFT and CI levels of theory.

In this work we compute the spectroscopic constants of the $^1\Sigma^+$ and $^3\Sigma^+$ states of TiC at the CI level using large basis sets. The scalar relativistic and Ti core-valence effects are included.

2 Methods

We use a complete-active-space self-consistent-field (CASSCF) approach to optimize the orbitals. The Ti $3d$, $4s$, and $4p\sigma$ orbitals and the C $2s$ and $2p$ orbitals are in the active space. More extensive correlation is included using the internally contracted [4, 5] multireference configuration interaction (IC-MRCI)

approach. The effect of higher excitations is estimated using the multireference analog of the Davidson correction, which is denoted IC-MRCI+Q. The CASSCF configurations are used as references and, unless otherwise noted, only those electrons in the CASSCF active space are correlated at the IC-MRCI level. When two $^1\Sigma^+$ states are studied, a state-averaged CASSCF procedure is used.

The effect of Ti $3s$ and $3p$ correlation is investigated at several levels of theory. The first is the CASPT2 approach [6, 7, 8, 9]. The definition of the valence treatment is the same as in the MRCI treatment, while the core-valence calculations add the Ti $3s$ and $3p$ orbitals to the inactive space. That is, the valence and core-valence treatments use the same reference list. We use both the g_0 and g_1 Fock operators [10]. We should note that owing to intruder state problems, it was necessary to include a shift [11] of $0.2E_H$ in the CASPT2 calculations. The second approach is the CIPT2 method [12], where the active electrons are correlated at the CI level and the inactive electrons are correlated at the CASPT2 level. The same active and inactive spaces and reference lists are used as in the IC-MRCI and CASPT2 treatments. For the valence treatment, the CIPT2 approach reduces to the IC-MRCI approach. Finally we note that we consider the effect of $3s$ and $3p$ correlation on the dissociation energy of the $^3\Sigma^+$ state using the restricted coupled-cluster singles and doubles approach [13, 14], including the effect of connected triples determined using perturbation theory [15, 16], RCCSD(T). The CCSD(T) approach cannot be used for the $^1\Sigma^+$ state since it is not well described by a single reference.

Scalar relativistic effects are included using the Douglas–Kroll–Hess (DKH) approach [17, 18]. In the nonrelativistic calculations, the Ti (21s16p9d6f4g)/[7s6p4d3f2g] averaged atomic natural orbital [19] and the C augmented-correlation-consistent polarized valence triple zeta [20, 21] (aug-cc-pVTZ) sets are used. In the DKH calculations, the primitives from the aug-cc-pVTZ set are contracted in the same manner as in the nonrelativistic calculations, except the contraction coefficients are taken from an atomic DKH calculation. For Ti, the (21s13p8d) basis set optimized by Partridge [22] is used. To this we add the three p and one d supplemental functions optimized by Partridge. In addition, diffuse s (0.009) and p (0.005) functions are added. Excluding the diffuse s and p functions, this primitive set is the same as that used in the nonrelativistic calculations. The Ti set is contracted using a DKH calculation for the ground 3F state. The first 16 s primitive functions are contracted to three functions, the first ten p primitives are contracted to two functions, and the first four d primitives are contracted to one function, while the remaining primitives are uncontracted. The averaged atomic natural orbital (6f4g)/[3f2g] polarization set is used [19] in the DKH calculations. The calculations were performed using MOLPRO [23, 24] which was modified to compute the DKH integrals.

3 Results and discussion

We summarize our results in Table 1 along with some previous work. A plot of the two $^1\Sigma^+$ IC-MRCI+Q potentials is given in Fig. 1. We should note that if the active space did not include the Ti $4p\sigma$ orbital, we were unable to obtain smooth potentials for the two $^1\Sigma^+$ states in the region shown in the figure.

The first set of IC-MRCI calculations does not include the scalar relativistic effects, and these yield a $^3\Sigma^+$ ground state. The r_e and dipole moment are similar to the previous MRCI values [2]. Our ω_e value is larger than the previous MRCI result, but in reasonable agreement with the BPW91/6-311+G* results. The $(1)^1\Sigma^+$ state is dominated by a $\sigma^1\sigma'^1$ occupation, while the $(2)^1\Sigma^+$ state is dominated by a σ^2 occupation. The results for the $(1)^1\Sigma^+$ state are similar for the one- and two-state treatments; the one-state treatment is expected to be the more accurate of the two. Our $(1)^1\Sigma^+$ r_e and dipole moment values are in reasonable agreement with the previous MRCI results. Our ω_e value is larger, as found for the triplet state, and our computed T_e is smaller than those found previously. Our $(2)^1\Sigma^+$ state r_e and dipole moment values are in reasonable agreement with those obtained with the DFT approaches. This is not too surprising because the DFT solution corresponds to the same σ^2 occupation as found for the $(2)^1\Sigma^+$ state. The $(2)^1\Sigma^+$ IC-MRCI+Q ω_e value is significantly larger than that found at the DFT level, presumably because the MRCI solution is forced to be orthogonal and noninteracting with the lower $^1\Sigma^+$, which changes the shape of the potential.

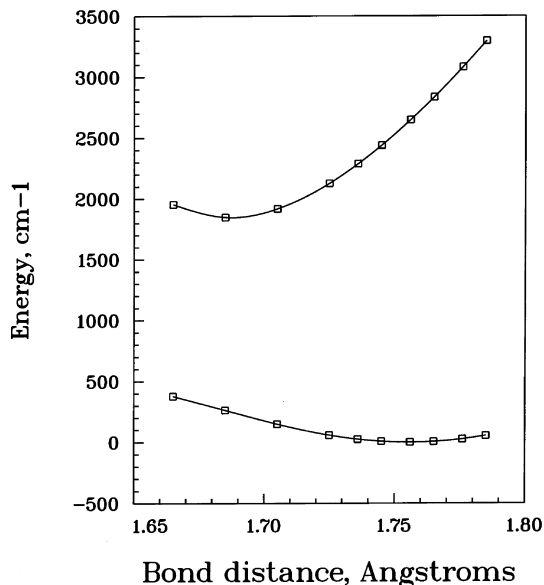


Fig. 1. The IC-MRCI+Q potentials for the two lowest $^1\Sigma^+$ states

We also include the results for the $^3\Pi$ state, which is much lower in energy than that previously reported [3], but is not a candidate for the ground state. The difference with previous work arises because the $^3\Pi$ state is best described as arising from a $8\sigma^2 9\sigma^1 3\pi^3$ occupation, whereas an occupation of $8\sigma^1 3\pi^4 4\pi^1$ was assumed previously.

Table 1. Summary of computed TiC spectroscopic constants

State	$r_e(\text{\AA})$	$\omega_e(\text{cm}^{-1})$	$T_e(\text{cm}^{-1})$	$\mu(\text{D})$
IC-MRCI+Q				
$^3\Sigma^+$	1.723	848	0	2.57 ^a
$(1)^1\Sigma^+$ (one-state treatment)	1.774	740	351	2.36 ^a
$(1)^1\Sigma^+$ (two-states treatment)	1.756	677	286	2.93 ^a
$(2)^1\Sigma^+$ (two-states treatment)	1.687	1239	2134	6.03 ^a
$^3\Pi$	1.786	771	4184	
DKH-IC-MRCI+Q				
$^3\Sigma^+$	1.721	855	0	2.67 ^a
$(1)^1\Sigma^+$ (one-state treatment)	1.774	753	286	2.38 ^a
$(1)^1\Sigma^+$ (two-states treatment)	1.765	725	312	2.72 ^a
$(2)^1\Sigma^+$ (two-states treatment)	1.670	1212	2546	6.84 ^a
DKH-CIPT2				
$^3\Sigma^+$	1.698	894	0	
$(1)^1\Sigma^+$ (one-state treatment)	1.746	786	1134	
DKH-CIPT2+Q				
$^3\Sigma^+$	1.704	881	0	
$(1)^1\Sigma^+$ (one-state treatment)	1.754	767	1071	
Previous work				
MRCI ^b				
$^3\Sigma^+$	1.735	704	0	2.73
$^1\Sigma^+$	1.790	592	1253	2.16
B3LYP ^b				
$^3\Sigma^+$	1.668	988	0	3.16
$^1\Sigma^+$	1.607	980	546	6.63
BPW91 ^b				
$^3\Sigma^+$	1.679	972	0	3.02
$^1\Sigma^+$	1.641	924	-518	5.79
BPW91/6-311+G* ^c				
$^3\Sigma^+$	1.705	891	0	2.96
$^1\Sigma^+$	1.637	921	-887	5.92

^a Computed as an expectation value at the MRCI level

^b Reference [2]

^c Reference [1]

Table 2. The effect of the number electrons correlated on the $^1\Sigma^+ - ^3\Sigma^+$ separation (cm^{-1}). The separation was computed at $r(^1\Sigma^+) = 1.774 \text{ \AA}$ and $r(^3\Sigma^+) = 1.723 \text{ \AA}$

Calculation	Valence	Core–valence	Δ
DKH-CASSCF	555		
DKH-IC-MRCI ^a	358	1139	781
DKH-IC-MRCI+Q ^a	285	1072	786
DKH-CASPT2	636	1394	758
DKH-CASPT2(g1)	467	1217	750

^a The core–valence value was computed using the CIPT2 method

Table 3. The dissociation energy of the $^3\Sigma^+$ state of TiC (eV)

	Valence	Core–valence	Δ
DKH-IC-MRCI ^a	3.43	3.65	0.22
DKH-IC-MRCI+Q ^a	3.47	3.69	0.22
CCSD(T)	3.39	3.62	0.23
Experiment [25]		4.37 ± 0.31	

^a The core–valence value was computed using the CIPT2 method

The effect of scalar relativity on the computed spectroscopic constants is quite small. Adding Ti 3s and 3p correlation decreases the r_e values and increases the ω_e and T_e values; compare the IC-MRCI+Q and CIPT2+Q results in Table 1. The effect of Ti 3s and 3p correlation on the $^1\Sigma^+ - ^3\Sigma^+$ separation as a function of method is considered in more detail in Table 2. At the IC-MRCI/CIPT2 and IC-MRCI+Q/CIPT2+Q levels, the inclusion of Ti 3s and 3p correlation increases the separation by about 780-cm^{-1} . This is very similar to the about 750-cm^{-1} increase observed at the CASPT2 level for either the g0 or the g1 Fock operator. This is especially interesting in light of the fact that the $^1\Sigma^+ - ^3\Sigma^+$ separation at the valence CASPT2 level differs from the MRCI+Q by a few hundred reciprocal centimeters, with the default g0 Fock operator actually having a separation larger than that found at the CASSCF level. Since the change in separation when 3s and 3p correlation is included is very similar at the MRCI/CIPT2 and CASPT2 levels of theory, we can be confident that Ti 3s and 3p correlation increases the $^1\Sigma^+ - ^3\Sigma^+$ separation. Thus, while the reduction in the $^1\Sigma^+ - ^3\Sigma^+$ separation between the CASSCF and MRCI and between MRCI and MRCI+Q levels suggests that higher levels of electron correlation will lower the $^1\Sigma^+$ state relative to the $^3\Sigma^+$ state, the core-valence calculations show that Ti 3s and 3p correlation has a larger effect in the opposite direction. Using a two-state treatment at the CASPT2 level we test the possibility that core-valence correlation leads to an inversion of the $(1)^1\Sigma^+$ and $(2)^1\Sigma^+$ states. We find that core valence correlation lowers the $(2)^1\Sigma^+$ state by 880-cm^{-1} with respect to the $(1)^1\Sigma^+$ state but does not lead to an inversion. Therefore we conclude that the ground state is $^3\Sigma^+$ despite the small separation between the $^3\Sigma^+$ and $^1\Sigma^+$ states.

In Table 3 we compare our computed D_0 values with experiment [25]. The valence level values are in good mutual agreement, but are 0.9–1 eV smaller than

experiment. The inclusion of Ti 3s and 3p correlation increases D_0 by about 0.2 eV. Thus our best computed values are about 0.7 eV smaller than experiment, although it should be noted that experiment does have sizable error bars. While higher levels of theory will increase the computed values, we feel that it is unlikely that our error is 0.7 eV, and, therefore, we suggest that the true answer must lie at the lower end of the experimental range, if not lower.

4 Conclusions

The current calculations confirm that the ground state of TiC is $^3\Sigma^+$, as found previously using MRCI calculations. The calculations show that the difference in the r_e , ω_e , and μ values computed at the DFT and CI levels arises because the DFT methods are describing the closed-shell-like $(2)^1\Sigma^+$ state and not the $(1)^1\Sigma^+$ state, which is better described as an open-shell singlet. The computed D_0 values are smaller than experiment, and it is suggested that the true value lies at the lower end of the experimental range.

References

- Gutsev GL, Andrews L, Bauschlicher CW (2003) *Theor Chem Acc* 109: 299
- Hack MD, Maclagan RGAR, Scuseria GE, Gordon MS (1996) *J Chem Phys* 104: 6628
- Bauschlicher CW, Siegbahn PEM (1983) *Chem Phys Lett* 104: 331
- Werner H-J, Knowles PJ (1988) *J Chem Phys* 89: 5803
- Knowles PJ, Werner H-J (1988) *Chem Phys Lett* 145: 514
- Andersson K, Malmqvist P-Å, Roos BO, Sadlej A, Wolinski K (1990) *J Phys Chem* 94: 5483
- Andersson K, Malmqvist P-Å, Roos BO (1992) *J Chem Phys* 96: 1218
- Werner H-J (1996) *Mol Phys* 89: 645
- Celani P, Werner H-J (2000) *J Chem Phys* 112: 5546
- Andersson K (1995) *Theor Chim Acta* 91: 31
- Roos BO, Andersson K (1995) *Chem Phys Lett* 245: 215
- Celani P, Werner H-J, Knowles PJ (to be published)
- Bartlett RJ (1981) *Annu Rev Phys Chem* 32: 359
- (a) Knowles PJ, Hampel C, Werner H-J (1993) *J Chem Phys* 99: 5219; (b) Erratum (2000) *J Chem Phys* 112: 3106
- Raghavachari K, Trucks GW, Pople JA, Head-Gordon M (1989) *Chem Phys Lett* 157: 479
- Watts JD, Gauss J, Bartlett RJ (1993) *J Chem Phys* 98: 8718
- Douglas M, Kroll NM (1974) *Ann Phys* 82: 89
- Hess BA (1986) *Phys Rev A* 33: 3742
- Bauschlicher CW (1995) *Theor Chim Acta* 92: 183
- Dunning TH (1989) *J Chem Phys* 90: 1007
- Kendall RA, Dunning TH, Harrison RJ (1992) *J Chem Phys* 96: 6796
- Partridge H (1989) *J Chem Phys* 90: 1043
- Werner H-J, Knowles PJ, MOLPRO, version 2002. (a package of ab initio programs) with contribution by Amos RD, Bernhardsson A, Berning A, Celani P, Cooper DL, Deegan MJO, Dobbyn AJ, Eckert F, Hampel C, Hetzer G, Korona T, Lindh R, Lloyd AW, McNicholas SJ, Manby FR, Meyer W, Mura ME, Nicklass A, Palmieri P, Pitzer R, Rauhut G, Schütz M, Schumann U, Stoll H, Stone AJ, Tarroni R, Thorsteinsson T, Lindh R, Ryu U, Liu B (1991) *J Chem Phys* 95: 5889
- Gupta SK, Gingerich KA (1980) *High Temp-High Pressure* 12: 273